A recently identified member of the glutathione transferase structural family modifies cardiac RyR2 substate activity, coupled gating and activation by Ca^{2+} and ATP

Angela F. DULHUNTY[1], Pierre POULIQUIN, Marjorie COGGAN, Peter W. GAGE and Philip G. BOARD
Division of Molecular Bioscience, John Curtin School of Medical Research, P.O. Box 334, Canberra, ACT 2601, Australia

The recently discovered CLIC-2 protein (where CLIC stands for chloride intracellular channel), which belongs to the ubiquitous glutathione transferase structural family and is expressed in the myocardium, is a regulator of native cardiac RyR2 (ryanodine receptor 2) channels. Here we show that recombinant CLIC-2 increases [^{3}H]ryanodine binding to native and purified RyR channels, enhances substate activity in individual channels, increases the number of rare coupled gating events between associated RyRs, and reduces activation of the channels by their primary endogenous cytoplasmic ligands, ATP and Ca^{2+}. CLIC-2 (0.2–10 μM) added to the cytoplasmic side of RyR2 channels in lipid bilayers depressed activity in a reversible, voltage-independent, manner in the presence of activating (10–100 μM) or sub-activating (100 nM) cytoplasmic Ca^{2+} concentrations. Although the number of channel openings to all levels was reduced, the fraction and duration of openings to substate levels were increased after exposure to CLIC-2. CLIC-2 reduced increases in activity induced by ATP or adenosine 5′-[β,γ-imido]triphosphate. Depression of channel activity by CLIC-2 was greater in the presence of 100 μM cytoplasmic Ca^{2+} than with 100 nM or 10 μM Ca^{2+}. Further, CLIC-2 prevented the usual ~50-fold increase in activity when the cytoplasmic Ca^{2+} concentration was increased from 100 nM to 100 μM. The results show that CLIC-2 interacts with the RyR protein by a mechanism that does not require oxidation, but is influenced by a conserved Cys residue at position 30. CLIC-2 is one of only a few cytosolic inhibitors of cardiac RyR2 channels, and may suppress their activity during diastole and during stress. CLIC-2 provides a unique probe for substate activity, coupled gating and ligand-induced activation of cardiac RyR channels.

Key words: CLIC-2, CLIC (chloride intracellular channel) protein, coupled gating, cytoplasmic Ca^{2+} and Mg^{2+}, ryanodine receptor Ca^{2+} channel.

INTRODUCTION

RyR (ryanodine receptor) Ca^{2+} channels are responsible for Ca^{2+} release from internal stores in skeletal and cardiac muscle during EC (excitation–contraction) coupling. Ca^{2+} entering through voltage-dependent L-type Ca^{2+} channels triggers Ca^{2+} release in cardiac muscle, while a protein–protein interaction between the L-type Ca^{2+} channel and the skeletal RyR (RyR1) initiates EC coupling in skeletal muscle [1]. Ca^{2+} and protein–protein interactions with surface membrane ion channels can also activate RyRs in non-muscle cells [2,3].

The RyR is an unusual ligand-gated ion channel, because its ability to open is modulated by several cellular components, including Mg^{2+} and ATP, and by associated proteins such as the FKBPs (FK506 binding proteins) [4,5], calmodulin [6,7], Ca^{2+}/calmodulin kinase II [8] and Homer [9]. The channel's activity is altered by covalent modification by oxidation/reduction, nitrosylation and phosphorylation [3]. ATP and Ca^{2+} are the two major activators of the cardiac RyR2. ATP is required in addition to Ca^{2+} for the channels to achieve an open probability close to 1.0, which occurs during EC coupling [10,11]. RyR activity must fall to reduce Ca^{2+} release and maintain the Ca^{2+} store when the muscle is not contracting. The resting activity of skeletal RyR1 is low because the channel is strongly inhibited by Mg^{2+} [12]. However, cardiac RyR2 channels are not inhibited by Mg^{2+} at normal cytosolic concentrations [13], and an important and unresolved question is the mechanism that maintains low activity of RyR2 channels during relaxation. A novel inhibitor of RyR2, expressed in cardiac muscle, is CLIC-2 (where CLIC stands for chloride intracellular channel) [14].

The recently recognized CLIC family of proteins are grouped together on the basis of sequence similarity, but their functions are not well defined. The proteins are named CLIC because the first to be described formed intracellular chloride channels [15]. Although CLIC-2 is found in several tissues, including skeletal muscle and myocardium, the only function attributed to it thus far is cardiac RyR inhibition [14]. Since it is one of only a few known endogenous inhibitors of cardiac RyRs, it is important to understand the mechanisms by which CLIC-2 alters channel gating. The present study of the effects of CLIC-2 on the cardiac RyR2 channel, and its activation by ATP and by Ca^{2+}, have yielded several novel results. The protein when added to the cytoplasmic (*cis*) solution (a) alters the gating of the channels by reducing the number of openings, increasing the fraction of openings to substate levels and increasing the probability of rare coupled gating events, and (b) depresses the normal increase in activity in response to ATP and Ca^{2+}. We also show that CLIC-2 interacts with the RyR by a mechanism that does not involve covalent modification. CLIC-2 profoundly alters the activity of cardiac RyR2 channels, and is a useful probe for gating mechanisms within and between the channels.

Abbreviations used: AEBSF, 4-(2-aminoethyl)benzenesulphonyl fluoride; BAPTA, bis-(*o*-aminophenoxy)ethane-*N*,*N*,*N*′,*N*′-tetra-acetic acid; CLIC, chloride intracellular channel; DTT, dithiothreitol; EC coupling, excitation–contraction coupling; FKBP, FK506 binding protein; GST, glutathione transferase; I_{max}, maximum single-channel current; p[NH]ppA, adenosine 5′-[β,γ-imido]triphosphate; RyR, ryanodine receptor; SR, sarcoplasmic reticulum.

[1] To whom correspondence should be addressed (email Angela.dulhunty@anu.edu.au).

EXPERIMENTAL

Expression and purification of recombinant CLIC-2

Human CLIC-2 was expressed in *Escherichia coli* with a residual N-terminal poly-His tag that facilitated the purification of the recombinant protein. The coding sequence was amplified from the EST (expressed sequence tag) clone AI129485 and ligated between the BamHI and PstI sites in the pQE-30 vector (Qiagen, Clifton Hills, SA, Australia) and transformed into *E. coli* M15[pREP4] host cells. The primers used for the amplification were CLIC2ExSBF (5′-CTCCGCGGTGGATCCGGCCT-GCGGCCCGGCACT-3′) and CLIC2ExPR (5′-TTGCATGCTG-CAGCCTGTAAGAGCTCTCCT-3′), and contained BamHI and PstI sites respectively. The resulting cDNA clone, pQECLIC2, was re-sequenced to exclude amplification errors.

A culture of pQECLIC2 in M15[pREP4] cells was grown overnight in the presence of 0.1 mM isopropyl β-D-thiogalactoside and processed as described in [16]. The recombinant protein was purified by immobilized metal affinity chromatography with nickel–agarose, as described for other His-tagged GSTs (glutathione transferases) [16], with the exception that buffer A (50 mM sodium phosphate/300 mM NaCl) was adjusted to pH 7.0 and the purified enzyme was dialysed against 5 mM Hepes or 50 mM Hepes, plus either 10 % (v/v) glycerol or 200 mM NaCl, pH 7. For some preparations, the recombinant CLIC-2 was purified further by gel filtration on a Pharmacia FPLC Superose 12 column equilibrated with 50 mM Hepes/10 % glycerol, pH 7.0.

To determine if Cys residues at positions 30 and 33 in CLIC-2 play a role in the modulation of RyR2, we used a Quik Change Site-Directed Mutagenesis Kit (Stratagene, La Jolla, CA, U.S.A.) to mutate them individually to Ala. The mutations were checked by DNA sequencing (Biological Resource Facility, John Curtin School of Medical Research). The two mutated proteins, CLIC-2 C30A and CLIC-2 C33A, were expressed and purified by the same methods used for the wild-type protein. Both the wild-type and mutant CLIC-2 proteins were added to bilayers or ryanodine binding solutions at concentrations between 0.2 and 20 μM, shown previously to be effective in reducing channel activity [14].

Anti-CLIC-2 antibody

Antiserum was raised in a New Zealand White rabbit using purified His-tagged CLIC-2 with Freund's adjuvant and a standard immunization protocol.

SDS/PAGE and Western blotting

Both CLIC-2 (1 μg) and microsomal (P4) fractions from sheep heart (15 μg) were run together on a 5–17 % (w/v) polyacrylamide gradient gel and stained with Coomassie Brilliant Blue. Proteins were transferred on to Immobilon-P PVDF transfer membranes, and probed first with the anti-CLIC-2 antibody (see above). The second antibody was horseradish peroxidase-conjugated anti-rabbit Ig (P0448; Dako Corp., Carpinteria, CA, U.S.A.).

RyR isolation and purification, and incorporation into liposomes

SR (sarcoplasmic reticulum) vesicles were prepared from sheep heart [17]. All steps were performed at 4 °C. RyR was purified from solubilized SR vesicles using a sub-continuous sucrose gradient (modified from [18]). Gradient and solubilization solutions contained 25 mM NaPipes, pH 7.4, 1 M NaCl, 1 mM DTT (dithiothreitol), 0.5 % (w/v) CHAPS, 0.25 % (w/v) L-α-phosphatidylcholine (Avanti), 100 μM EGTA, 92 μM $CaCl_2$, 500 μM AMP and protease inhibitors recommended by the provider (Roche 'Complete' tablet). Sucrose gradients were made of four 7.5 ml layers [5 %, 10 %, 15 % and 20 % (w/v) sucrose], and kept for 6 h before use. SR vesicles were homogenized in solubilization solution at a final protein concentration of 2.5 $mg \cdot ml^{-1}$ and centrifuged for 20 min at 120 000 ***g*** (Beckman rotor TLA 100.3). Supernatant (4 ml) was loaded on to the sucrose gradient and centrifuged overnight at 64 000 ***g*** into a Beckman SW28 rotor. Fractions (2 ml) were collected, and RyR-enriched fractions were identified on silver-stained SDS/PAGE. Selected fractions were concentrated ~10-fold using a Vivaspin 2 concentrator (Vivascience) and protein concentration was determined by DC protein assay (Bio-Rad). RyR content was confirmed by SDS/PAGE and [^{3}H]ryanodine binding. The gels showed some protein equivalent to the Ca^{2+}-ATPase in the RyR-containing fractions, but very little (if any) lower-molecular-mass material. The 12-fold increase in [^{3}H]ryanodine binding per mg of protein (see Table 1) is indicative of significant removal of other lower-molecular-mass proteins during purification. The solubilized fractions were snap-frozen and stored at − 70 °C.

To incorporate solubilized RyR into liposomes, phosphatidylethanolamine (200 μl), phosphatidylcholine (60 μl) and phosphatidylserine (60 μl) (Avanti) were mixed and dried under nitrogen, and then 200 μl of solubilized fraction and 66 μl of 400 mg/ml CHAPS were added. The mixture was sonicated for 10 min at 4 °C and dialysed overnight at 4 °C against 10 mM NaPipes (pH 7.4), 0.5 M NaCl, 1 mM DTT, 2.6 mM AEBSF [4-(2-aminoethyl)benzenesulphonyl fluoride], 100 μM EGTA and 200 μM $CaCl_2$. The liposomes were centrifuged at 120 000 ***g*** for 20 min at 4 °C, and the pellets were resuspended in 10 mM NaPipes (pH 7.4), 0.25 M NaCl, 1 mM DTT, 2.6 mM AEBSF, 100 μM EGTA and 200 μM $CaCl_2$, snap-frozen and stored at − 70 °C. Before use, liposomes were thawed slowly at room temperature, frozen and thawed again three times, and/or sonicated for 20 s at 4 °C (three times).

Lipid bilayers and solutions

Bilayers were formed and vesicles incorporated as described in [19]. SR vesicles (10 μg/ml), purified protein or protein in liposomes was added to the *cis* chamber using *cis* and *trans* solutions containing 20 mM CsCl, 1.0 mM $CaCl_2$ and 10 mM Tes (pH 7.4 adjusted with CsOH), as well as either *cis*/*trans* 230/230 mM methane sulphonate plus 500/0 mM mannitol or 230/30 mM methane sulphonate (no mannitol). Channel activity was recorded with symmetrical 250/250 mM Cs^+. Ca^{2+} was buffered to 100 nM and 10 μM with 2 mM BAPTA [bis-(*o*-aminophenoxy)ethane-*N*,*N*,*N*′,*N*′-tetra-acetic acid]. The potential difference across the bilayer is expressed as $V_{cis} - V_{trans}$ (i.e. $V_{cytoplasm} - V_{lumen}$).

Recording and analysis of single-channel data

This was performed as described in [19]. Channel activity was recorded at + 40 and − 40 mV to determine whether the actions of CLIC-2 were voltage-dependent. The bilayer potential was switched from one potential to the other every ⩾30 s throughout the experiment. Solutions were exchanged by perfusion using back-to-back syringes. The efficiency of exchange was determined spectrophotometrically at 710 nm, by dilution of 1 mM Antipyrylazo III (in distilled water) during perfusion with different volumes of distilled water. Perfusion with 11 ml of solution (~ 6 vol.) gave ~ 10 000-fold dilution.

Gross fluctuations in baseline current were corrected with an in-house program ('Baseline', developed by Dr D. R. Laver). Estimates of channel activity were based on measurements of both

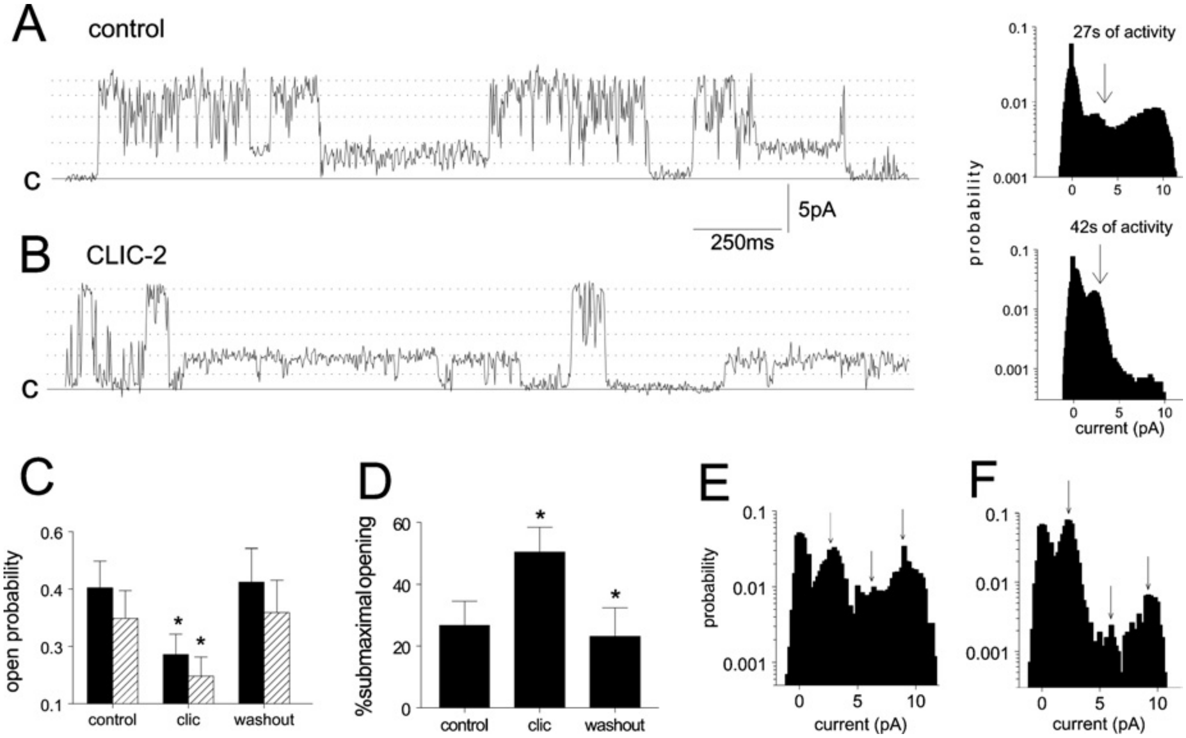

Figure 1 CLIC-2 in the *cis* solution reversibly decreases the activity of Ca^{2+}-activated cardiac RyR2 channels, by reducing the number of open events and by increasing the fraction of events to substate levels

The *cis* [Ca^{2+}] was 10 μM. Panels (**A**) and (**B**) show 2.5 s segments of activity, and all-points histograms for 27 s and 42 s recordings, at +40 mV under control conditions and after addition of 0.5 μM CLIC-2 respectively. The recordings were selected to illustrate substate levels. Broken lines are through prominent current levels at 17 %, 38 %, 57 %, 77 % and 100 % of I_{max} (10.5 pA). Continuous lines (c) show the closed current level. The histograms for 27 s (control) and 42 s (CLIC-2) of activity show a net fall in activity and an increased fraction of substate openings in the presence of CLIC-2, especially at 38 % I_{max} (arrow). (**C**, **D**) Analysis of eight experiments in which one channel only was active (with periods of occasional high conductance activity in four of them excluded) and clear substate openings. More than 120 s of activity (more than four 30 s segments) at +40 mV were analysed for control, CLIC-2 (clic) and post-perfusion (washout) conditions (CLIC-2 was added at concentrations between 0.2 and 10 μM). (**C**) Solid bars show the probability of channel openings to levels greater than ~2 pA (P_o), and hatched bars show the probability of channel opening to the maximum single channel conductance [P_o(max)]. (**D**) Percentage of channel openings to substate levels under each condition. (**E**, **F**) All-point histograms for selected segments of activity in (**A**) and (**B**) respectively.

mean current (I') and the channel parameters (open probability, and mean open and closed times), measured using the software package Channel2 (developed by Professor P. W. Gage and M. Smith). Mean current is the average of all data points in a recording; (a) it includes openings to all substate levels and (b) it can be used when more than one channel is open in the bilayer. On the other hand, measurement of open probability depends on setting threshold levels for channel opening at ~2 pA, and for channel closing between the open threshold and the baseline. This analysis excluded small substate openings of less than 2 pA.

To estimate the fraction of channel openings to substate levels, the probability of single channel openings to all levels greater than 2 pA (P_o) was measured. Then the threshold discriminator was set just below the maximum single-channel current (I_{max}) to determine the probability of openings only to I_{max} [P_o(max)]. The percentage of subconductance openings was given by $100 \times [P_o - P_o(\max)]/P_o$. Conventional single-channel analysis was not possible when channels were strongly activated (10 μM *cis* Ca^{2+} plus 2 mM ATP, or 100 μM *cis* Ca^{2+}) because, although only one channel was active under other conditions, additional channels opened under these strongly activating conditions. An indication of the effects of Ca^{2+} or ATP was obtained from the open probability and open and closed durations, without taking the number of channels in the bilayer into consideration. The parameters were true single-channel parameters for all conditions, except with 10 μM *cis* Ca^{2+} plus 2 mM ATP or with 100 μM *cis* Ca^{2+}.

Probability of simultaneous channel openings

High-conductance openings to levels corresponding to the simultaneous opening of three channels (3^*I_{max}) were occasionally observed in recordings in which no other openings exceeded I_{max}. To determine whether these high conductance openings were due to coupled gating between one active channel and two otherwise silent channels, or to the random simultaneous opening of three separate channels, we looked at the probability of rapid transitions between the closed level and I_{max} (‘rapid transitions’ occurred within a sample period of 2 ms or four data points at a sample rate of 2 kHz with a filter of 1 kHz). The probability of one channel opening (P_1) was then the number of rapid transitions (N_1) divided by the number of sample periods (e.g. 10000 for a 20 s recording). Twenty rapid transitions in a 20 s recording gave $P_1 = 2 \times 10^{-3}$. The probability of three simultaneous random events within the same period (P_3) was then $P_1{}^3$, i.e. 8×10^{-9} (essentially zero). If the number of rapid transitions from the closed level to 3^*I_{max} exceeded $P_1{}^3$ by a significant amount, they could not be attributed to random events. This analysis is based on [20].

[^{3}H]Ryanodine binding

SR vesicles (50 μg of protein) or purified RyR (5 μg of protein) were incubated with 15 nM [^{3}H]ryanodine ([9,21(n)-^{3}H]-ryanodine; Amersham Biosciences) in 40 mM Pipes, pH 7.4, 200 mM KCl, 1 mM BAPTA and sufficient $CaCl_2$ to give 10 μM free Ca^{2+} (confirmed with a Ca^{2+} electrode), in a final

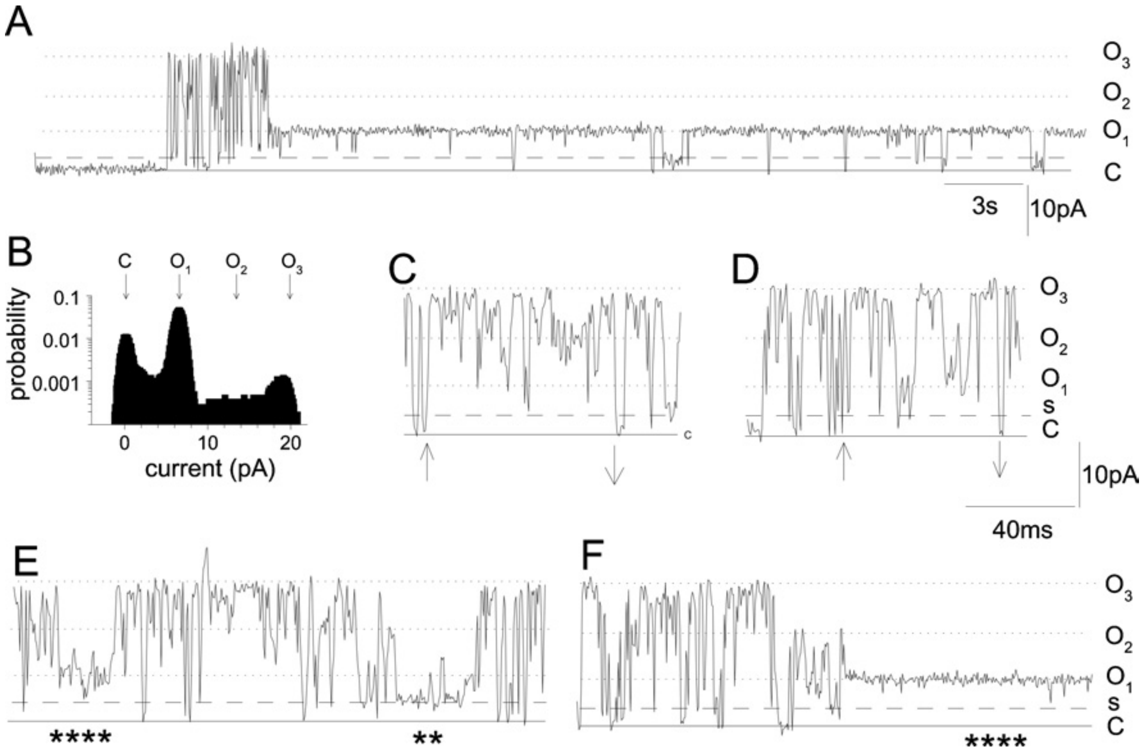

Figure 2 Occasional coupled gating events

Occasional synchronized openings to 3*I_{max} were observed. (**A**) A 30 s recording with a brief burst of such openings and an otherwise high probability of opening to I_{max} obtained in the presence of 0.2 μM CLIC-2. (**B**) All-points histogram for the recording with peaks at the closed level (C), I_{max} (O_1), and 3*I_{max} (O_3), as indicated by arrows, as well as the 2*I_{max} (O_2) level, which does not appear as a sharp peak. Panels (**C**) and (**D**) show 100 ms of activity with rapid transitions between C (closed level) and 3*I_{max} (up arrows), and 3*I_{max} and C (down arrows), separated by transitions between the three open levels. Panels (**E**) and (**F**) show 230 ms of activity with frequent transitions between C (closed level) and 3*I_{max} and each of the open levels, as well as long openings to the single-channel substate (s) (**) and to I_{max} (****). In (**A**) and (**C**)–(**F**), the solid line shows the closed level, the dotted lines show O_1, O_2 and O_3, and the dashed line shows a level at ~40 % I_{max} which is assumed to be a single-channel substate (s).

volume of 125 μl. Samples incubated overnight at 24 °C were diluted with 1 ml of ice-cold 200 mM KCl. Purified RyR protein was precipitated by poly(ethylene glycol) [21]. Samples were filtered through Whatman GF/F filters preincubated in 1 % (v/v) poly(ethyleneimine). Filters were washed (3 × 4 ml) with ice-cold 200 mM KCl, and radioactivity was determined by liquid scintillation counting. Non-specific binding was determined using a 1000-fold excess of non-radioactive ryanodine. Results in Table 1 are means from at least three different experiments, each performed in triplicate, using preparations from at least two different sheep hearts.

Statistical analysis of data

Results from 5–10 bilayers were measured for each set of experiments. Data are given as means ± S.E.M., and were tested for significance ($P < 0.05$) with Student's t test or a non-parametric 'sign' test.

RESULTS

Channels were characterized as RyRs because they (a) had a Cs^+ conductance of 200–250 pS (typical when *trans* [Ca^{2+}] is 1 mM [22]), (b) were activated at *cis* (cytoplasmic) [Ca^{2+}] between 1 and 100 μM, and/or by 2 mM *cis* ATP {or its non-hydrolysable analogue p[NH]ppA (adenosine 5′-[β,γ-imido]triphosphate)}, and (c) were inhibited by 30 μM Ruthenium Red. The presence of RyRs was also confirmed by [^{3}H]ryanodine binding.

Effects of CLIC-2 on RyR2 channel gating

CLIC-2 inhibits cardiac RyR2 and prolongs substate openings

Reduced activity in the presence of CLIC-2 was due to a fall in the overall number of channel openings, and to an increase in the fraction of openings to submaximal conductance levels (Figure 1) in 90 of 95 experiments. In contrast, substate activity increased in only five of 46 channels after adding either vehicle (buffer) or anti-CLIC-2 antibody in the absence of CLIC. The conductance of the substate levels was not changed by CLIC-2, but some openings were prolonged (Figure 1). There were predominant levels at ~20 % and 40 % of the maximum conductance (I_{max}) (Figure 1). Other levels commonly observed were at ~60 % and ~80 % of I_{max}.

Occasional coupled gating events

Occasional high-conductance openings were observed in a subset of experiments (Figure 2): in five of 46 experiments in the absence of CLIC-2, and in 30 of 95 experiments with CLIC-2 (described here, reported previously [14] or yet to be published). The openings were in brief bursts lasting 0.3–4 s, which occurred only between one and four times in experiments lasting up to 40 min. The maximum current during the burst was 3 times the single-channel current (3*I_{max}). These rare high-conductance openings were observed with P_o values of ~0.01 to 0.5, were observed only at +40 mV (never −40 mV), and were not time-locked to changes in potential. The high-conductance events were analysed in eight experiments in which all other openings were to

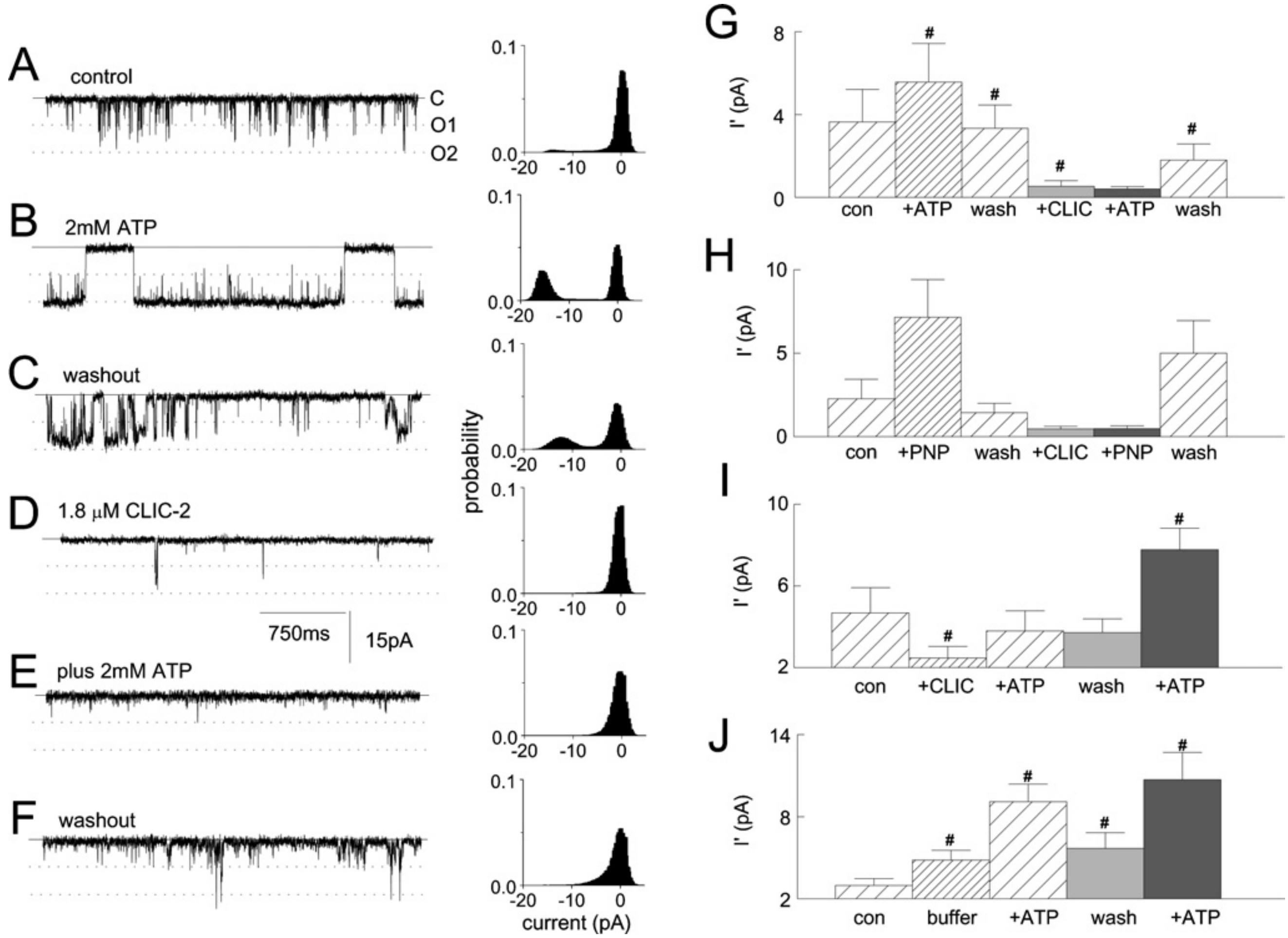

Figure 3 ATP-induced activation of RyR2 is prevented by CLIC-2

(**A**)–(**F**) Recordings (3 s) and all-points histograms (60 s; two 30 s recordings), in the presence of 10 μM *cis* Ca^{2+}, for control conditions (**A**), after adding 2 mM ATP (**B**), after washout of ATP (**C**), after adding 2.4 μM CLIC-2 (**D**), after adding 2.4 μM CLIC-2 and then 2 mM ATP (**E**), and after washout of ATP and CLIC-2 (**F**). Channels open downward from closed (continuous line) to single (O_1) or double (O_2) open levels (dotted lines). (**G**, **H**) Average mean current (I'). Data at -40 and $+40$ mV were combined for six experiments with ATP (**G**) and two with p[NH]ppA (**H**) ($n = 4$ observations). Means $\pm$ S.E.M. are given for ATP, and means $\pm$ S.D. are given for p[NH]ppA, under control conditions (con), after 2 mM ATP (+ATP in **G**) or p[NH]ppA (+PNP in **H**), after washout (wash), after adding 2.1–4.5 μM CLIC-2 (+CLIC), after adding CLIC-2 plus 2 mM ATP (+ATP in **G**) or p[NH]ppA (+PNP in **H**), and after a second washout (wash). (**I**, **J**) Reversibility and specificity of CLIC-2. Data at -40 and $+40$ mV were combined for eight experiments with 2.1–4.5 μM CLIC-2 (in 40–80 μl of vehicle, i.e. 50 mM Hepes buffer plus 10 % glycerol, pH 7) (**I**) and seven experiments with 40–80 μl of buffer alone (**J**). Values are means $\pm$ S.E.M. for control (con), after adding CLIC-2 (**I**) or buffer (**J**), then after adding ATP, after washout, and finally after adding 2 mM ATP in the absence of CLIC-2. # indicates significant difference from the preceding condition.

I_{max} (Figure 2). The events were thought to reflect coupled gating between one active RyR and two otherwise silent RyRs, for the following reasons. (a) No other openings in the recording exceeded I_{max}, even when P_o was high. (b) Transitions between the closed level (0 pA) and either I_{max} or 3^*I_{max} occurred within four data points (at 500 μs/point) (Figure 2). (c) Fast openings from 0 pA to 3^*I_{max} were followed by multiple transitions between I_{max}, 2^*I_{max} and 3^*I_{max} before a fast closing from 3^*I_{max} back to 0 pA (Figure 2). (d) Fast transitions from closed to 3^*I_{max} exceeded the probability of three simultaneous random openings. For example, in the 30 s recording in Figure 2(A), there were 17 fast transitions from 0 pA to I_{max}. The probability of three random transitions to 3^*I_{max} was 1.45×10^{-9}, yet there were 47 such transitions.

In an average analysis period of 6.4 ± 3.5 s ($n = 8$), 19.6 ± 7.9 fast transitions to 3^*I_{max} were observed. Since the observed probability of fast transitions to I_{max} was $(2 \pm 0.6) \times 10^{-2}$, the predicted probability of random transitions to 3^*I_{max} was $(2 \pm 1) \times 10^{-5}$. Since the number of observed transitions to 3^*I_{max} was significantly greater than the probability of random openings, this indicates that the fast openings to 3^*I_{max} were coupled.

We suggest (see Discussion) that vesicles incorporated into bilayers contain many RyRs, and that all but one are silent in single-channel recordings. The rare coupled gating events may occur between three of the channels, and may be related to coupled gating observed by others [23]. It is clear that the probability of the events was enhanced by CLIC-2 but, in our hands, the events were too irregular for further experimentation.

Effects of CLIC-2 on RyR2 activation by ATP and Ca^{2+}

CLIC-2 reduces activation of RyR2 by ATP

Channel activity increased when ATP was added, and fell when it was removed after brief exposures (Figure 3). After adding CLIC-2, ATP failed to activate the channel, although activity increased when CLIC-2 and ATP were removed (Figures 3A–3F). Average data with ATP or p[NH]ppA showed the same trends (Figures 3G and 3H).

The prevention of ATP-induced activation was reversible, since channels were activated by ATP when CLIC-2 was perfused from the solution (Figure 3I). Since the order of application of ATP

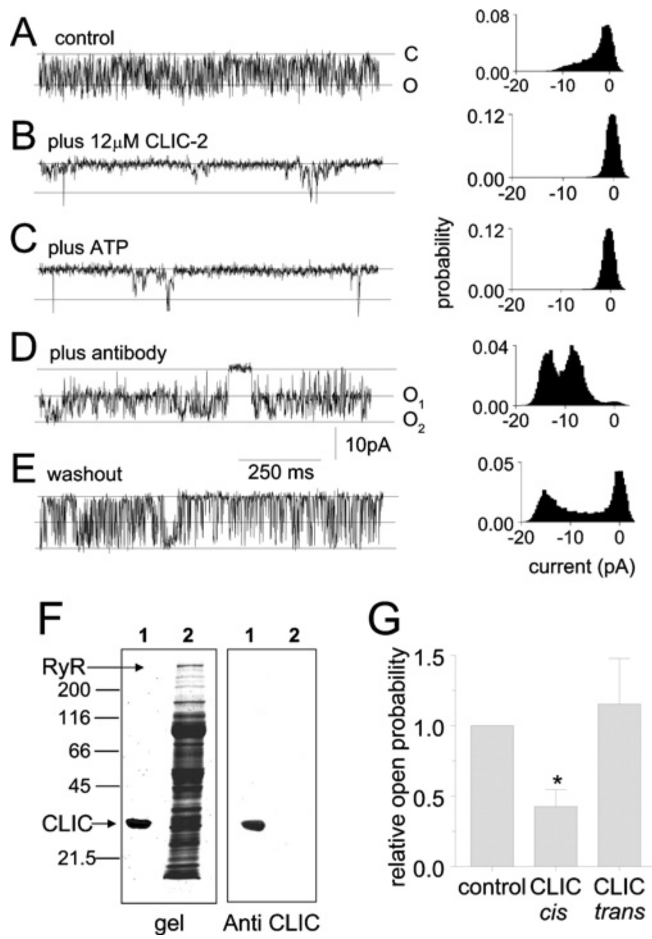

Figure 4 Anti-CLIC-2 antibody prevents the effect of CLIC-2 on ATP-induced activation

The recordings show 1 s of continuous activity and all-points histograms for 60 s of channel activity (two 30 s recordings) with *cis* [Ca^{2+}] = 10 μM under control conditions (**A**), after adding 12 μM CLIC-2 (**B**), then 2 mM ATP (**C**), then 5 μl of antibody (**D**), and finally after washout of ATP, antibody and CLIC-2 (**E**). Channel opening is downward from the closed level (continuous line) to the maximum single-channel conductance (dotted line). Opening of a second channel is seen in (**D**) and (**E**): the first dotted line (O_1) is I_{max} and the second dotted line (O_2) is I when the two channels are open. (**F**) Coomassie Blue-stained gel (left panel) and after staining with the anti-CLIC antiserum (right panel). Arrows point to the high-molecular-mass RyR2 and the lower-molecular-mass CLIC-2. The positions of selected molecular mass markers are shown on the left in kDa. CLIC-2 lies just above the 31 kDa marker. (**G**) Relative open probability under control conditions, and after adding 7 μM CLIC-2 to the *cis* chamber ($n = 4$ experiments) or the *trans* chamber ($n = 5$ experiments).

and CLIC-2 was reversed in Figures 3(G) and 3(I), the effects were not due to time-dependent changes in gating, or effects of ATP or CLIC-2 on phosphorylation or oxidation. Neither were the effects due to the CLIC-2 vehicle (50 mM Hepes/10 % glycerol buffer, pH 7) (Figure 3J). The similar actions of ATP and its non-hydrolysable analogue p[NH]ppA indicate that CLIC-2 acts on the ligand binding of ATP, not on phosphorylation [8].

A polyclonal antibody to CLIC-2 prevents inhibition of RyR2 by CLIC-2 [14]. The antibody eliminated the effects of CLIC-2 on ATP-induced activation (Figure 4). The antibody binds strongly to CLIC-2, but did not interact with the RyR or with any other protein in the SR vesicles in Western blot analysis (Figure 4F) or ELISA (results not shown). A control experiment confirmed that CLIC-2 inhibits RyR activity only when added to the *cis* (cytoplasmic) chamber, but not when added to the *trans* (luminal) side of the RyR (Figure 4G). Channel analysis showed that CLIC-2 (a) reduced the open probability and duration of openings to I_{max} and increased closed times, and (b) prevented ATP-induced changes in channel gating (Figure 5). Although the effect of ATP was greatest at −40 mV, CLIC-2 had similar effects at −40 and +40 mV.

CLIC-2 reduces the activation of RyR2 by cytoplasmic Ca^{2+}

The effect of CLIC-2 on the increase in activity of RyR2 when *cis* [Ca^{2+}] was increased from 100 nM to 100 μM was examined. Control activity with sub-activating 100 nM *cis* [Ca^{2+}] was low ($P_o = 0.009 \pm 0.002$; $n = 22$). Nevertheless, there were still fewer openings after adding CLIC-2 (Figures 6A and 6B). Increasing *cis* [Ca^{2+}] to 100 μM then increased activity, but to a lesser extent than in the same channels after washout of CLIC-2 (Figures 6C–6F). The reduced response was not due either to the channel responding more to a second exposure to 100 μM Ca^{2+} or to an effect of vehicle (Figures 6F and 6G). These results suggest that a part of the inhibitory effect of CLIC-2 on Ca^{2+}-activated channels was depression of Ca^{2+}-induced activation. In the absence of CLIC-2, 100 μM Ca^{2+} caused large increases in open probability and open duration, and a decrease in closed duration (Figures 7A and 7B). In the presence of CLIC-2, the increase in open probability was smaller, there was no significant increase in open duration, and the decrease in mean closed times was less.

Channel activity was reduced to ~50 % of control by CLIC-2 when *cis* [Ca^{2+}] was 100 nM or 10 μM, and to ~12 % when *cis* [Ca^{2+}] was 100 μM (Figure 7C). Mean current in the presence of CLIC-2 with 100 μM *cis* Ca^{2+} was significantly lower than with 10 μM *cis* Ca^{2+}. Thus the action of CLIC-2 was Ca^{2+}-dependent and more effective at higher Ca^{2+} concentrations.

CLIC-2 interactions with solubilized RyR2 and [^{3}H]ryanodine binding

CLIC-2 reduced maximal openings in solubilized RyRs and increased substate activity (Figure 8). Similar results were obtained in seven cases in which solubilized protein was incorporated into the bilayer, and four of five cases when solubilized channels in liposomes were incorporated. The conductance of the solubilized channels was greater than that of native channels, but remained within the range reported for RyR2, which can increase above 500 pS. The activity of solubilized channels remained sensitive to Ruthenium Red. Other changes in RyR2 properties have been reported after solubilization [13].

[^{3}H]Ryanodine binding also indicated an interaction between CLIC-2 and native or solubilized RyRs (Table 1). Ryanodine binding to native vesicles and solubilized RyRs was enhanced by ~30 % in the presence of 19 μM CLIC-2. The increased binding was seen under a variety of conditions, including pH 6.8, free [Ca^{2+}] from 10 nM to 100 μM, EGTA instead of BAPTA, Cs^+ instead of K^+, in the absence of AESBF, and with CLIC-2 concentrations ranging from 1 to 19 μM. Thus the effect of CLIC-2 did not depend on the conditions of the assay. Ryanodine binding to CLIC-2 alone was not detected.

Effects of mutant CLIC-2 on RyR channels

A cysteine residue at position 30 is conserved in CLIC-1–CLIC-5 and aligns with the active-site Cys in GSTO1 [24]. Unlike the other CLIC proteins, CLIC-2 has an additional Cys at position 33 that forms part of a CPFC (Cys-Pro-Phe-Cys) motif, similar to the CPYC and CPSC motifs in the active sites of human glutaredoxins 1 and 2 [25]. If these two Cys residues formed a disulphide bond and played a role in redox reactions, their removal would alter the reactions. Channel activity was reduced by 6.7 μM CLIC-2

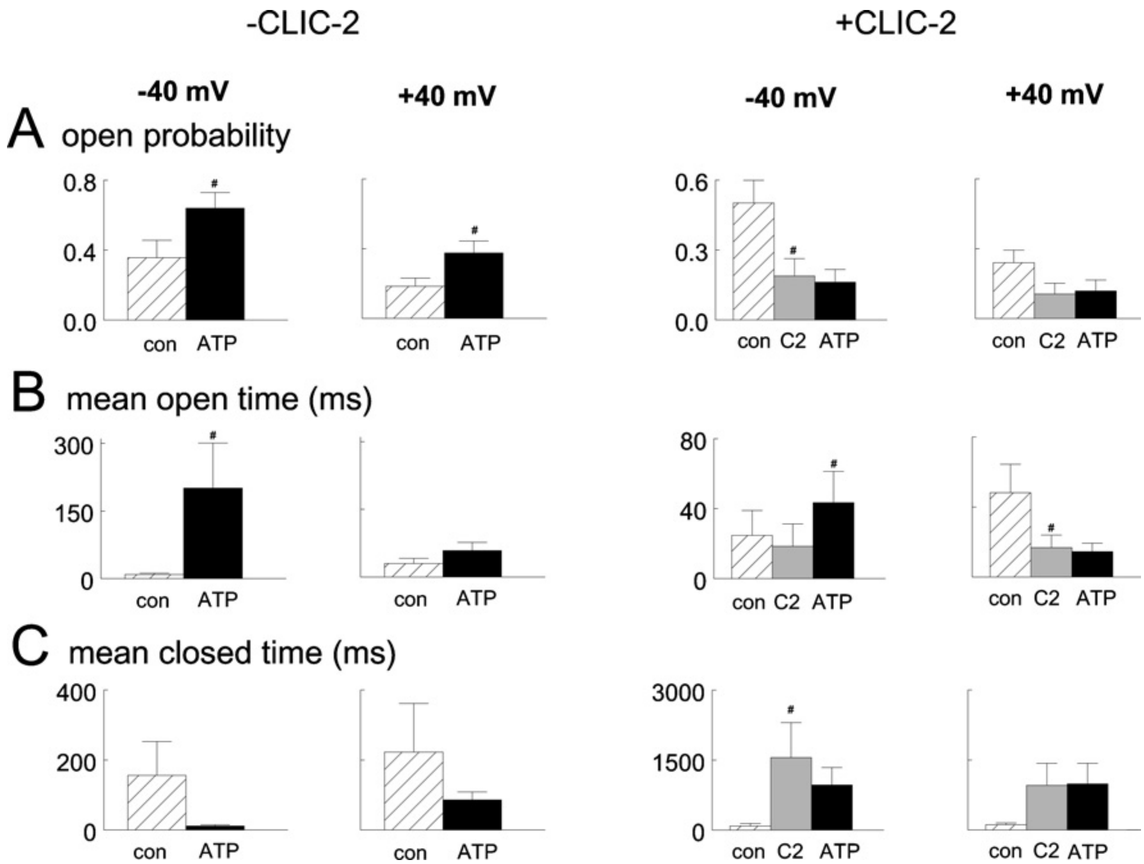

Figure 5 Effects of ATP on current parameters in the absence and presence of CLIC-2

Each group of two histograms shows average parameters at −40 mV (left) and +40 mV (right). The data are given as means ± S.E.M. for open probability (**A**), mean open time (**B**) and closed time (**C**). Data in the absence of CLIC-2 are shown under control conditions with 10 μM *cis* Ca^{2+} (con) and after addition of 2 mM ATP (ATP). Data in the presence of CLIC-2 are shown under control conditions (con) and after addition of 4–12 μM CLIC-2 (C2) or CLIC-2 plus 2 mM ATP (ATP). # indicates significant difference from the preceding condition.

Table 1 [^{3}H]Ryanodine binding to native SR vesicles and purified RyR channels

Binding was carried out in the presence of 10 μM free Ca^{2+}. The results are presented as specific activity, in pmol of ryanodine bound per mg of protein; relative binding (%) is given in parentheses. The values are averages ± S.E.M. for five observations under each condition; $*P < 0.05$ compared with control. CLIC-2 (19 μM) was added both to SR vesicles and to purified RyRs.

RyR	Control	CLIC-2
SR vesicles	1.03 ± 0.12 (100 %)	1.35 ± 0.13* (130 %)
Purified RyR	12.5 ± 1.38 (100 %)	16.24 ± 1.95* (130 %)

C30A mutant in five of eight experiments with native RyR2 and one of seven experiments with solubilized RyR2, and by 5.4 μM CLIC-2 C33A mutant in three of three native RyR2 experiments and five of five solubilized RyR2 experiments. In all cases, the reduction in maximal opening was accompanied by increased substate activity. There was no change in substate activity in the three channels that were not affected by CLIC-2 C30A. In the same series of experiments, 8.6 μM wild-type CLIC-2 inhibited maximal opening and enhanced substate activity of native RyR2 in five of five experiments and of solubilized RyR2 in nine of ten experiments. Thus, although the C30A mutation reduced the interaction of CLIC-2 with RyR2 channels, neither of the two cysteine residues is an essential determinant of the effects of CLIC-2, indicating that the action of CLIC-2 does not depend on their modifying the redox state of the channels.

DISCUSSION

We have previously described an interaction between CLIC-2 and RyR2, and shown that CLIC-2 is expressed in cardiac muscle [14]. This is the first report of complex interactions between CLIC-2 and the intrinsic gating mechanisms of cardiac RyR2 channels and their regulation by endogenous activators. CLIC-2 increases [^{3}H]ryanodine binding, increases the fraction of channel openings to substate levels and increases the probability of coupled channel openings. On the other hand, CLIC-2 reduces RyR2 activation by ATP or Ca^{2+}, and suppresses 'leak' currents at resting cytoplasmic Ca^{2+} concentrations. CLIC-2 is one of the few physiological inhibitors of RyR2; it (a) has the potential to prevent Ca^{2+} store depletion in the heart, and (b) provides a novel probe for substate and coupled gating in RyR2 channels.

Effects of CLIC-2 on substate activity and coupled gating

Subconductance openings in RyR channels are enhanced by diverse compounds [4,5,26–30]. Some studies suggest that the channel can assume four conductance levels which are correlated with the four RyR subunits [4,5,31], while others show a multitude of conductance levels [32]. Both CLIC-2 and FKBP12 promote coupled gating of RyRs and influence substate activity.

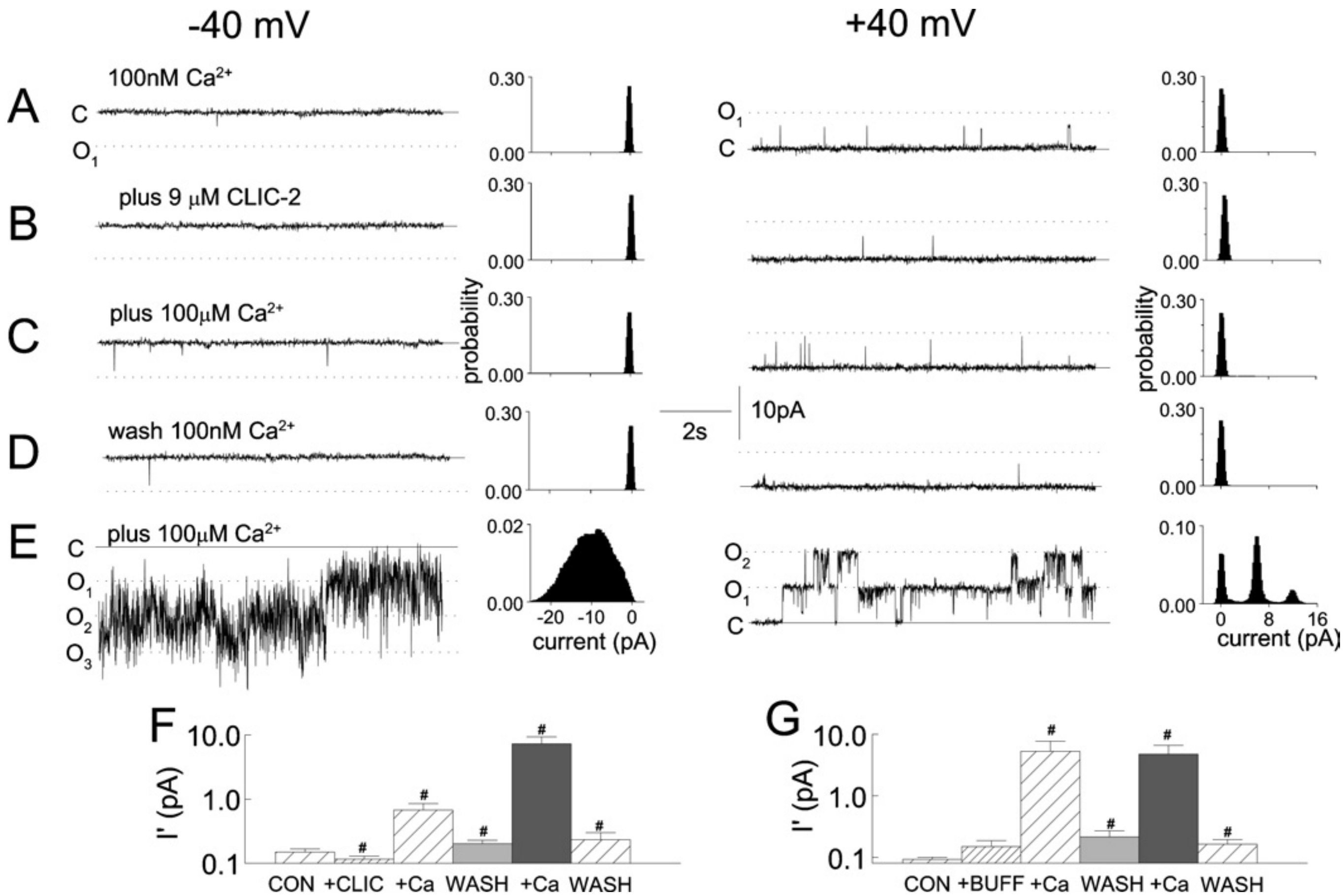

Figure 6 CLIC-2 inhibits RyR2 at resting cytoplasmic Ca^{2+} concentrations and reduces Ca^{2+}-induced activation of the channel

Panels (**A**)–(**E**) show 10 s recordings and all-points histograms for 60 s of activity (two 30 s recordings), at +40 mV (left panels) and −40 mV (right panels). *Cis* [Ca^{2+}] was 100 nM under control conditions. In (**A**)–(**D**), channels opened from the closed level (C; continuous line) to the maximum single-channel conductance (O_1; dotted line). In the last recording in each panel, openings of one, two or three channels can be seen to levels O_1, O_2 and O_3 respectively in the recordings and histograms. Recordings are shown under control conditions (**A**), with 9 μM CLIC-2 (**B**), after increasing *cis* [Ca^{2+}] to 100 μM (**C**), after washout and return to 100 nM *cis* Ca^{2+} (**D**), and then after addition of 100 μM Ca^{2+} in the absence of CLIC-2 (**E**). (**F**, **G**) Data at −40 and +40 mV are combined for 11 experiments with 9 μM CLIC-2 (in 50 μl of vehicle, i.e. 50 mM Hepes buffer plus 200 mM NaCl, pH 7.5) (**F**) ($n = 22$ observations) and for six experiments with 50 μl of buffer alone (**G**) ($n = 12$ observations). The bars show averages ± S.E.M. of the mean current (I'), with 100 nM *cis* Ca^{2+} (CON), with 2–9 μM CLIC-2 [or 50 μl of buffer alone (BUFF)], after increasing [Ca^{2+}] to 100 μM (+Ca), and after washout. # indicates significant difference from the preceding condition.

Coupled gating is seen in several channel types [23,33–36]. The coupled openings in our present study were always to 3^*I_{max}, implying either that there are three RyRs in a vesicle or that coupling occurs preferentially between three channels. Vesicles probably contain more than three channels, because parallel rows of RyRs extend for several hundred nanometres along the junctional face membrane [37]. If 25 % of the circumference of a 600 nm vesicle [38] is junctional face membrane, it would include around eight RyRs in a double row [37,39]. Indeed, electron micrographs show several RyRs in one vesicle [38], and 4–50 channels can be observed after one vesicle incorporation into bilayers (D. R. Laver, personal communication). Thus most channels are silent even with mild Ca^{2+} activation, but can open during strong activation (Figure 6). Coupled gating described in [23,35], also in ~10 % of RyRs, differed from that here, in that (a) it was continuous, not in brief bursts, and (b) it was between two channels, not three. If coupling involves RyR aggregation, CLIC-2 may bridge RyRs or uncover association sites. Alternatively, if RyRs retain their two-dimensional crystalline geometry in the bilayer, CLIC-2 could facilitate cross-talk between channels. Coupled gating with CLIC-2 increases current through RyRs and opposes the inhibitory effect on full openings. Since bursts to 3^*I_{max} occurred only at positive potentials (which could develop during Ca^{2+} release), CLIC-2 may co-ordinate RyR2 openings during EC coupling, while depressing Ca^{2+} release under resting conditions. A reduced ‘leak’ through RyRs at rest would help maintain low cytoplasmic Ca^{2+} concentrations during diastole.

Ca^{2+}-dependence of the effects of CLIC-2

The ability of CLIC-2 to reduce activation by *cis* Ca^{2+} and ATP would allow the protein to prevent regenerative Ca^{2+} release following spontaneous release events (sparks) that occur during diastole [40]. To speculate further, the Ca^{2+}-dependence of CLIC-2 is such that the protein caused the greatest depression of activity when the RyR is maximally Ca^{2+}-activated by 100 μM *cis* Ca^{2+}. Thus CLIC-2 may also act to terminate Ca^{2+} release once channel activity has peaked. Maximum activation of RyR2 by Ca^{2+} occurs only in the presence of ATP [10,11]. The depression of ATP-induced activation by CLIC-2 would facilitate its termination of high rates of Ca^{2+} release, and would also help to maintain low Ca^{2+} release during diastole. The complex actions of CLIC-2 endow the protein with the potential to facilitate high rates of

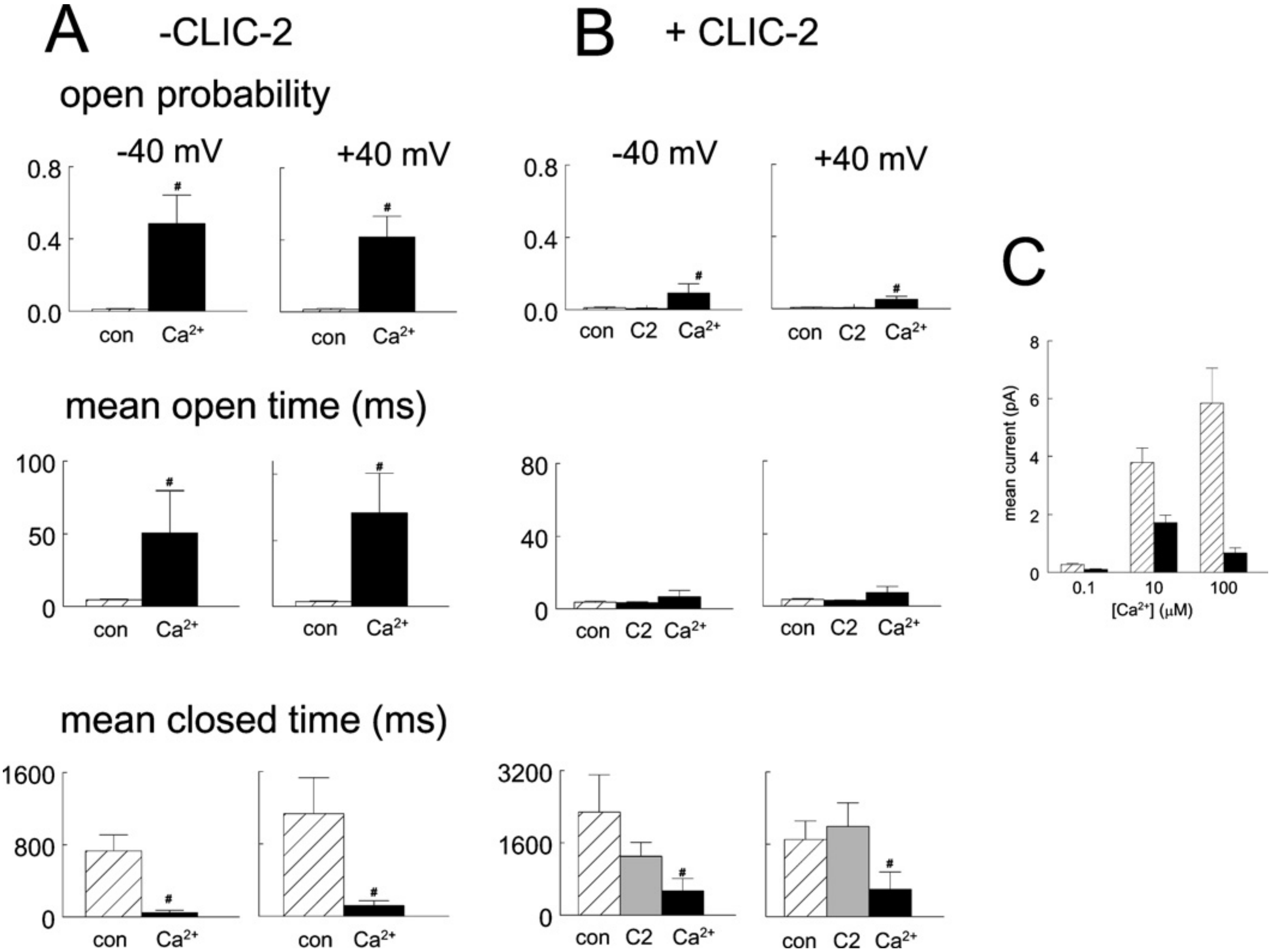

Figure 7 Effects of increasing the *cis* Ca^{2+} concentration from 100 nM to 100 μM on current parameters in the absence and presence of CLIC-2

(**A**, **B**) Each group of two histograms shows average parameters at −40 mV (left) and +40 mV (right). Data are shown as means + S.E.M. In the absence of CLIC-2, control data with 100 nM *cis* Ca^{2+} (con) and data with 100 μM Ca^{2+} (Ca^{2+}) are shown. Data with CLIC-2 are control with 100 nM *cis* Ca^{2+} (con), after addition of 2–9 μM CLIC-2 (C2), and in the presence of CLIC-2 plus 100 μM Ca^{2+} (Ca^{2+}). # indicates significant difference from the preceding condition. (**C**) Data at different Ca^{2+} concentrations, in the presence (solid bars) or absence (hatched bars) of 0.2–12 μM CLIC-2, plotted as a function of [Ca^{2+}]. In the absence of CLIC-2, $n = 100$ for 100 nM Ca^{2+}, $n = 42$ for 10 μM Ca^{2+} and $n = 38$ for 100 μM Ca^{2+}. In the presence of CLIC-2, $n = 22$ for 100 nM Ca^{2+}, $n = 12$ for 10 μM Ca^{2+} and $n = 22$ for 100 μM Ca^{2+}.

Ca^{2+} release during diastole, then to terminate Ca^{2+} release and maintain low release during systole.

Interaction of CLIC-2 with the cardiac RyR complex

CLIC-2 inhibits RyR2 by binding specifically to the cytoplasmic side of the channel complex. No inhibition was seen when the protein was added to the luminal side. It is not clear whether CLIC-2 exerts its multiple actions by binding to a single site on the cytoplasmic domain of the RyR complex, or to several sites. It is curious that CLIC-2 caused an overall depression of channel activity, yet increased [^{3}H]ryanodine binding. It is likely that [^{3}H]ryanodine binding reflects one or both of the potentially activating actions of CLIC-2, i.e. prolongation of substate activity and/or enhanced coupled gating. Since bilayer experiments look at short-term effects of drugs (5–10 min), while ryanodine binding proceeds for several hours, the activating effects of the protein may be more pronounced after longer exposures. Interestingly, the C30A mutation decreased the number of channels that were inhibited by CLIC-2. The Cys^{30} residue aligns with the active-site Cys^{32} in GSTO 1 [24], and C32A substitution in GSTO 1 abolishes the inhibitory effects of the GST on RyR2 [19]. Thus Cys^{30} may be in the CLIC-2 domain that interacts with RyR2.

Does CLIC-2 modulate the redox or the phosphorylation state of the channel?

The activity of RyRs is sensitive to both redox state and phosphorylation [3,41–43]. CLIC-2 is a member of the GST structural family [19], and some GSTs have thiol transferase activity [44], although CLIC-2 has little [14]. CLIC-2 does not modify RyR activity by either redox reactions or phosphorylation, since the effects of the protein are reversible within a few minutes of wash-out [14]. Further, removal of Cys residues that may covalently modify RyR2 does not abolish CLIC-2 activity. Finally, both high- and low-activity channels, that may be respectively oxidized or reduced [45], are equally susceptible to modification by CLIC-2. It remains to be determined whether the expression of CLIC-2, or its actions on the RyR, depend on the redox state. If the concentration or efficacy of CLIC-2 increased with oxidative stress, its inhibitory effects may help to reduce Ca^{2+} overload.

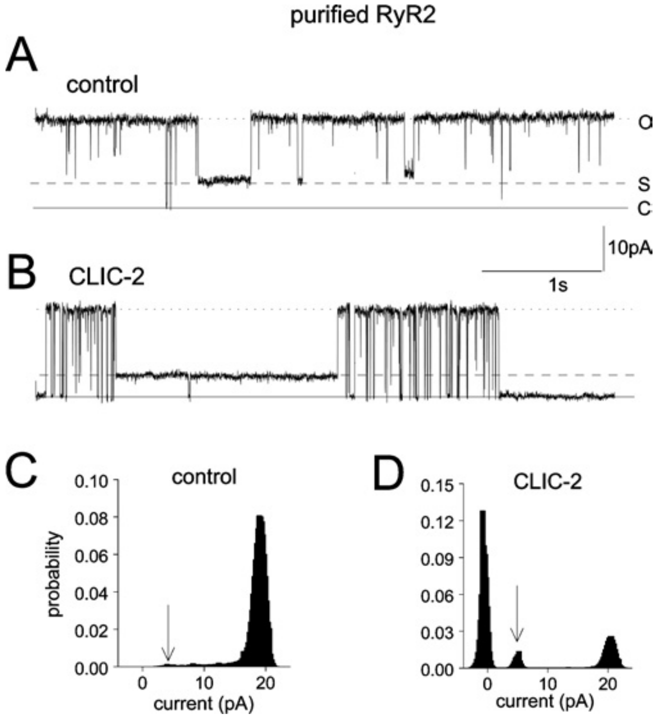

Figure 8 CLIC-2 decreases maximum channel openings and enhances substate activity in purified RyR channels

Panels (**A**) and (**B**) show 5 s current recordings from a single purified RyR channel at +40 mV, before (**A**) and after (**B**) the addition of 8.6 μM CLIC-2 (100 μl) to the *cis* solution. The closed current level is indicated by the solid line (C), I_{max} by the dotted line (O), and the dominant substate level by the broken line (S). (**C**, **D**) All-points histograms for 30 s of activity before (**C**) and after (**D**) addition of CLIC-2. The arrow in (**D**) points to the dominant substate level.

Conclusions

In summary, the work presented here shows that CLIC-2 reduces cardiac RyR2 channel activity when cytoplasmic Ca^{2+} is either resting or activating. Furthermore, CLIC-2 (a) enhanced [^{3}H]ryanodine binding to native and solubilized RyR2, (b) enhanced substate activity and coupled gating, and (c) altered the response of the cardiac RyR to the two endogenous regulators whose actions combine to increase the open probability of the RyR channel to high levels during EC coupling. These changes profoundly alter the functional responses of the RyR channel at rest and during EC coupling, and indicate a significant role for CLIC-2 in cardiac muscle *in vivo*.

We are grateful to Suzy Pace and Joan Stivala for their assistance with preparation and characterization of cardiac SR vesicles and purification of RyR2. We thank Sarah Watson, Gerlinde Lenz, Dane Cully, Suzanne Curtis and Esther Gallant for their assistance with bilayer experiments, and Damian Triffett for assistance with expression and purification of CLIC-2. We acknowledge financial support from Pfizer and a grant from the Australian National Health and Medical Research Council (#268027).

REFERENCES

1 Dulhunty, A. F., Haarmann, C., Green, D., Laver, D. R., Board, P. G. and Casarotto, M. G. (2002) Interactions between dihydropyridine receptors and ryanodine receptors in striated muscle. Prog. Biophys. Mol. Biol. **79**, 45–75

2 Mouton, J., Marty, I., Villaz, M., Feltz, A. and Maulet, Y. (2001) Molecular interaction of dihydropyridine receptors with type-1 ryanodine receptors in rat brain. Biochem. J. **354**, 597–603

3 Meissner, G. (1994) Ryanodine receptor/Ca^{++} release channels and their regulation by endogenous effectors. Annu. Rev. Physiol. **56**, 485–508

4 Brillantes, A.-M. B., Ondrias, K., Scott, A., Kobrinsky, E., Ondriasova, E., Moschella, M. C., Jayaraman, T., Landers, M., Ehrlich, B. E. and Marks, A. R. (1994) Stabilization of calcium release channel (ryanodine receptor) function by FK506-binding protein. Cell **77**, 513–523

5 Ahern, G. P., Junankar, P. R. and Dulhunty, A. F. (1994) Single channel activity of the ryanodine receptor calcium release channel is modulated by FK506. FEBS Lett. **352**, 369–374

6 Sencer, S., Papineni, R. V., Halling, D. B., Pate, P., Krol, J., Zhang, J. Z. and Hamilton, S. L. (2001) Coupling of RYR1 and L-type calcium channels via calmodulin binding domains. J. Biol. Chem. **276**, 38237–38241

7 Smith, J. S., Rousseau, E. and Meissner, G. (1989) Calmodulin modulation of single sarcoplasmic reticulum Ca^{++} release channels from cardiac and skeletal muscle. Circ. Res. **64**, 352–359

8 Dulhunty, A. F., Laver, D., Curtis, S. M., Pace, S., Haarmann, C. and Gallant, E. M. (2001) Characteristics of irreversible ATP activation suggest that native skeletal ryanodine receptors can be phosphorylated via an endogenous CaMKII. Biophys. J. **81**, 3240–3252

9 Feng, W., Tu, J., Yang, T., Vernon, P. S., Allen, P. D., Worley, P. F. and Pessah, I. N. (2002) Homer regulates gain of ryanodine receptor type 1 channel complex. J. Biol. Chem. **277**, 44722–44730

10 Kermode, H., Williams, A. J. and Sitsapesan, R. (1998) The interactions of ATP, ADP, and inorganic phosphate with the sheep cardiac ryanodine receptor. Biophys. J. **74**, 1296–1304

11 Xu, L., Mann, G. and Meissner, G. (1996) Regulation of cardiac Ca^{2+} release channel (ryanodine receptor) by Ca^{2+}, H^+, Mg^{2+}, and adenine nucleotides under normal and simulated ischemic conditions. Circ. Res. **79**, 1100–1109

12 Lamb, G. D. and Stephenson, D. G. (1991) Effect of Mg^{++} on the control of Ca^{++} release in skeletal muscle fibres of the toad. J. Physiol. (London) **434**, 507–528

13 Laver, D. R., Baynes, T. M. and Dulhunty, A. F. (1997) Magnesium inhibition of ryanodine-receptor calcium channels: evidence for two independent mechanisms. J. Membr. Biol. **156**, 213–229

14 Board, P. G., Coggan, M., Watson, S., Gage, P. W. and Dulhunty, A. F. (2004) CLIC-2 modulates cardiac ryanodine receptor Ca^{2+} release channels. Int. J. Biochem. Cell Biol. **36**, 1599–1612

15 Heiss, N. S. and Poustka, A. (1997) Genomic structure of a novel chloride channel gene, CLIC2, in Xq28. Genomics **45**, 224–228

16 Whittington, A., Vichai, V., Webb, G., Baker, R., Pearson, W. and Board, P. (1999) Gene structure, expression and chromosomal localization of murine theta class glutathione transferase mGSTT1-1. Biochem. J. **337**, 141–151

17 Laver, D. R., Roden, L. D., Ahern, G. P., Eager, K. R., Junankar, P. R. and Dulhunty, A. F. (1995) Cytoplasmic Ca^{2+} inhibits the ryanodine receptor from cardiac muscle. J. Membr. Biol. **147**, 7–22

18 Lee, H. B., Xu, L. and Meissner, G. (1994) Reconstitution of the skeletal muscle ryanodine receptor-Ca^{2+} release channel protein complex into proteoliposomes. J. Biol. Chem. **269**, 13305–13312

19 Dulhunty, A., Gage, P., Curtis, S., Chelvanayagam, G. and Board, P. (2001) The glutathione transferase structural family includes a nuclear chloride channel and a ryanodine receptor calcium release channel modulator. J. Biol. Chem. **276**, 3319–3323

20 Schneider, G. T., Cook, D. I., Gage, P. W. and Young, J. A. (1985) Voltage-sensitive, high-conductance chloride channels in the luminal membrane of cultured pulmonary alveolar (type II) cells. Pflugers Arch. **404**, 354–357

21 Glossmann, H. and Ferry, D. R. (1985) Assay for calcium channels. Methods Enzymol. **109**, 513–550

22 Tu, Q., Velez, P., Cortes-Gutierrez, M. and Fill, M. (1994) Surface charge potentiates conduction through the cardiac ryanodine receptor channel. J. Gen. Physiol. **103**, 853–867

23 Marx, S. O., Gaburjakova, J., Gaburjakova, M., Henrikson, C., Ondrias, K. and Marks, A. R. (2001) Coupled gating between cardiac calcium release channels (ryanodine receptors). Circ. Res. **88**, 1151–1158

24 Cromer, B. A., Morton, C. J., Board, P. G. and Parker, M. W. (2002) From glutathione transferase to pore in a CLIC. Eur. Biophys. J. **31**, 356–364

25 Gladyshev, V. N., Liu, A., Novoselov, S. V., Krysan, K., Sun, Q. A., Kryukov, V. M., Kryukov, G. V. and Lou, M. F. (2001) Identification and characterization of a new mammalian glutaredoxin (thioltransferase), Grx2. J. Biol. Chem. **276**, 30374–30380

26 Rousseau, E., Smith, J. S. and Meissner, G. (1987) Ryanodine modifies conductance and gating behaviour of single Ca^{++} release channel. Am. J. Physiol. **253**, C364–C368

27 Welch, W., Williams, A. J., Tinker, A., Mitchell, K. E., Deslongchamps, P., Lamothe, J., Gerzon, K., Bidasee, K. R., Besche, H. R., Airey, J. A. et al. (1997) Structural components of ryanodine responsible for modulation of sarcoplasmic reticulum calcium channel function. Biochemistry **36**, 2939–2950

28 Gurrola, G. B., Arevalo, C., Sreekumar, R., Lokuta, A. J., Walker, J. W. and Valdivia, H. H. (1999) Activation of ryanodine receptors by imperatoxin A and a peptide segment of the II-III loop of the dihydropyridine receptor. J. Biol. Chem. **274**, 7879–7886

29 Dulhunty, A. F., Curtis, S. M., Watson, S., Cengia, L. and Casarotto, M. G. (2004) Multiple actions of imperatoxin A on ryanodine receptors: interactions with the II-III loop "A" fragment. J. Biol. Chem. **279**, 11853–11862
30 Dulhunty, A. F., Laver, D. R., Gallant, E. M., Casarotto, M. G., Pace, S. M. and Curtis, S. (1999) Activation and inhibition of skeletal RyR channels by a part of the skeletal DHPR II-III loop: effects of DHPR Ser687 and FKBP12. Biophys. J. **77**, 189–203
31 Anyatonwu, G. I., Buck, E. D. and Ehrlich, B. E. (2003) Methanethiosulfonate ethylammonium block of amine currents through the ryanodine receptor reveals single pore architecture. J. Biol. Chem. **278**, 45528–45538
32 Hymel, L., Inui, M., Fleischer, S. and Schindler, H. (1988) Purified ryanodine receptor of skeletal muscle sarcoplasmic reticulum forms Ca^{2+}-activated oligomeric Ca^{2+} channels in planar bilayers. Proc. Natl. Acad. Sci. U.S.A. **85**, 441–445
33 Laver, D. R. and Gage, P. W. (1997) Interpretation of substates in ion channels: unipores or multipores? Prog. Biophys. Mol. Biol. **67**, 99–140
34 Everitt, A. B., Luu, T., Cromer, B., Tierney, M. L., Birnir, B., Olsen, R. W. and Gage, P. W. (2004) Conductance of recombinant GABA(A) channels is increased in cells co-expressing GABA(A) receptor-associated protein. J. Biol. Chem. **279**, 21701–21706
35 Marx, S. O., Ondrias, K. and Marks, A. R. (1998) Coupled gating between individual skeletal muscle Ca^{2+} release channels (ryanodine receptors). Science **281**, 818–821
36 Laver, D. R., O'Neill, E. R. and Lamb, G. D. (2004) Luminal Ca^{2+}-regulated Mg^{2+} inhibition of skeletal RyRs reconstituted as isolated channels or coupled clusters. J. Gen. Physiol. **124**, 741–758
37 Franzini-Armstrong, C. (1970) Studies of the triad. I. Structure of the junction in frog twitch fibers. J. Cell Biol. **47**, 488–498
38 Mitchell, R. D., Palade, P. and Fleischer, S. (1983) Purification of morphologically intact triad structures from skeletal muscle. J. Cell Biol. **96**, 1008–1016
39 Radermacher, M., Rao, V., Grassucci, R., Frank, J., Timerman, A. P., Fleischer, S. and Wagenknecht, T. (1994) Cryo-electron microscopy and three-dimensional reconstruction of the calcium release channel/ryanodine receptor from skeletal muscle. J. Cell Biol. **127**, 411–423
40 Cheng, H., Lederer, W. J. and Cannell, M. B. (1993) Calcium sparks: elementary events underlying excitation-contraction coupling in heart muscle. Science **262**, 740–744
41 Meissner, G. (2002) Regulation of mammalian ryanodine receptors. Front. Biosci. **7**, d2072–d2080
42 Dulhunty, A., Haarmann, C., Green, D. and Hart, J. (2000) How many cysteine residues regulate ryanodine receptor channel activity? Antioxid. Redox Signaling **2**, 27–34
43 Feng, W., Liu, G., Allen, P. D. and Pessah, I. N. (2000) Transmembrane redox sensor of ryanodine receptor complex. J. Biol. Chem. **275**, 35902–35907
44 Board, P. G., Coggan, M., Chelvanayagam, G., Easteal, S., Jermiin, L. S., Schulte, G. K., Danley, D. E., Hoth, L. R., Griffor, M. C., Kamath, A. V. et al. (2000) Identification, characterization, and crystal structure of the Omega class glutathione transferases. J. Biol. Chem. **275**, 24798–24806
45 Marengo, J. J., Hidalgo, C. and Bull, R. (1998) Sulfhydryl oxidation modifies the calcium dependence of ryanodine-sensitive calcium channels of excitable cells. Biophys. J. **74**, 1263–1277

Received 20 December 2004/9 May 2005; accepted 25 May 2005
Published as BJ Immediate Publication 25 May 2005, doi:10.1042/BJ20042113